Title	Analysis and Modeling of High-Power Phosphor-Coated White Light-Emitting Diodes With a Large Surface Area
Author(s)	Chen, H; Tan, SC; Hui, SYR
Citation	IEEE Transactions on Power Electronics, 2015, v. 30 n. 6, p. 3334-3344
Issued Date	2015
URL	http://hdl.handle.net/10722/209308
Rights	Creative Commons: Attribution 3.0 Hong Kong License

Analysis and Modeling of High-Power Phosphor-Coated White Light-Emitting Diodes With a Large Surface Area

Huan Ting Chen, *Member, IEEE*, Siew-Chong Tan, *Senior Member, IEEE*, and S.Y. R. Hui, *Fellow, IEEE*

***Abstract*—Modern high-power white light-emitting diodes (LEDs) composed of multiple blue LED chips and yellow phosphor coatings have been successfully commercialized because of their high-luminous efficacy. The multiple-chip LED packages usually come with flat structures that have large surface areas for considerable heat loss. Starting from the analysis and modeling of the blue LED chip, this paper introduces the thermal path through the phosphor layer to form the white phosphor-coated (PC) white LED device model for photometric, electric, and thermal performance analysis. The power distribution of the blue LED chip and that of the PC white LED device are compared. Based on this new analysis, the increase in the heat dissipation coefficient, equivalent thermal resistance, and power loss caused by the phosphor coating can be quantified. New equations suitable for device manufacturers to qualify their devices and design engineers to optimize LED system designs are derived. The analytical results are in good agreement with the practical mesurements.**

***Index Terms*—Light-emitting diodes, phosphor-coated white LEDs, photo-electro-thermal theory, thermal model.**

I. Introduction

THE combined use of yellow YAG:Ce phosphor and blue LED chip generates white light by mixing the two complementary colors. Such a combination has been the most common practice in modern high-power white LED packages. Usually, the phosphor layer is distributed uniformly on the surface of the blue LED chip. However, photons could be trapped inside the LED packages, especially if the packages are high power and compact. Therefore, more understanding is needed on the effects of the phosphor coating on the photometric, electric, and thermal performance of the white LED device.

In the phosphor layer, a fraction of the blue light undergoes the Stokes shift and the wavelength of the radiated light will slightly increase. Heat will be generated due to Stokes shift and light absorption [1], which can increase not only the chip junction temperature, but also the phosphor temperature.

Manuscript received February 23, 2014; revised May 5, 2014; accepted June 15, 2014. Date of publication July 8, 2014; date of current version January 16, 2015. This work was supported by the Hong Kong Research Grant Council through the Theme-based Research project: T22-715/12-N and by the National Natural Science Foundation of China under Grant 61307059. Recommended for publication by Associate Editor M. Ponce-Silva.

H. T. Chen and S-. C. Tan are with the Department of Electrical and Electronic Engineering, The University of Hong Kong, Hong Kong (e-mail: htchen23@gmail.com; sctan@eee.hku.hk).

S. Y. R. Hui is with the Department of Electrical and Electronic Engineering, The University of Hong Kong, Hong Kong, and also with Imperial College London, London SW7 2AZ, U.K. (e-mail: ronhui@eee.hku.hk).

Color versions of one or more of the figures in this paper are available online at http://ieeexplore.ieee.org.

Digital Object Identifier 10.1109/TPEL.2014.2336794

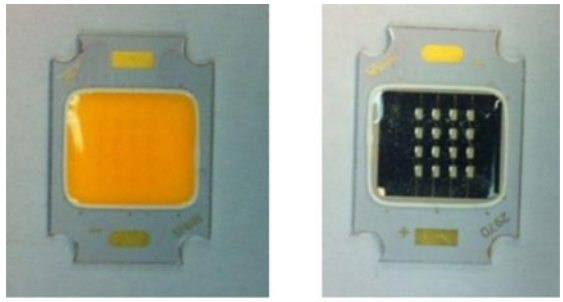

(a) (b)

Fig. 1. Photographs of two LED samples. (a) Blue LED (without yellow phosphor coating) and (b) PC white LED (with yellow phosphor coating intact).

Temperature is a key parameter affecting the lifetime [2]–[7], luminous efficacy [8]–[11], and color of the LED device and system [12]–[15]. For compact LED systems with devices closely packed together, improper device geometric arrangements on the heat sink and uneven heat distribution among LED devices can degrade both the LED device and the system's performance [2]. High temperature in the phosphor layer can result in the significant reduction of the phosphor emission caused by the thermal quenching effect [3]. Therefore, there is a challenge to determine how much heat is generated by the phosphor layer and to quantify the luminous flux reduction when designing the white LED devices and systems.

In this paper, two high-power LED samples of the same model and same batch are used for the investigation. Each LED sample composes of multiple blue LED chips and a yellow phosphor coating (under a transparent silicone cover). The first sample shown in Fig. 1(a) has the transparent silicone cover with the phosphor coating removed so that it is used as a blue LED for comparison. It is termed as "blue LED" in this paper. The second LED sample has the phosphor coating intact as shown in Fig. 1(b) and is termed as "PC white LED." It is important to note that such flat LED package design has a relatively large surface area for the heat flow as compared to that of a single chip package. In this paper, the heat flow through the phosphor coating and the silicone cover is analyzed and included in the model. The effects of the phosphor coating and the silicone cover on the photometric, electric, and thermal performance of the white LED package are studied and quantified. The heating power generated in the phoshpor layer and the luminous flux of the phosphor-coated (PC) white LED are evaluated theoretically and experimentally. Based on the photoelectrothermal theory and the use of the phosphor characteristics (absorption

coefficient of blue light of the phosphor layer, conversion coefficient of blue light converting into yellow light, and the phosphor thickness), the increase in the heat dissipation coefficient, the equivalent thermal resistance, and the power loss of the package arising from the phosphor material can be accurately quantified.

II. Electrical, Thermal, and Photometric Modeling of Blue LED and PC White LED

A. Electrical Diode Model Equations

The common electrical model for an LED consists of an ideal diode and a series resistance. The voltage V_D across the ideal diode can be expressed in terms of the total voltage drop V across the series combination of the ideal diode and the series resistance R_s. Thus, $V_D = V - IR_s$, and its current–voltage (*I–V*) characteristic is given by

$$I = C \exp\left[-\frac{E_g}{nkT_j}\right] \exp\left[\frac{q\,(V - IR_s)}{nkT_j}\right] \tag{1}$$

where I is the forward current of the LED, C is the device parameter, q is the magnitude of an electronic charge, k is the Boltzmann constant, T_j is the junction temperature, n is the ideality factor, and E_g is the bandgap energy.

The diode voltage equation is

$$V = IR_s + \frac{E_g}{q} + \frac{nkT_j}{q} \ln\left(\frac{I}{C}\right). \tag{2}$$

From (1) and (2), the diode power equation is, therefore

$$P_d = I^2 R_s + I\left[\frac{E_g}{q} + \frac{nkT_j}{q} \ln\left(\frac{I}{C}\right)\right]. \tag{3}$$

For (1)–(3), it is essential to determine the parameters such as E_g, n, and C. Using a Keithley 2400 SourceMeter in a four-wire setup, the current–voltage curve of an LED can be measured by placing the LED in a temperature-controlled oven under pulsed current injection with a small duty cycle. In this way, the self-heating of the p-n junction is negligible and, therefore, the junction temperature will be almost the same as the ambient temperature. The measured current–voltage curves for blue and PC white LED are shown in Figs. 2 and 3, respectively. Based on the measured results, the voltage equation in term of the current can be derived in the form of (2) by using piecewise linear iteration fitting (such as origin software) or genetic algorithm (such as MATLAB software). The physical device parameters in equation (2) should be automatically searched in a space of potential solutions through piecewise linear iteration fitting or genetic algorithm such that they finally reach an optimal set of solutions, which matches them to the measured curve, as depicted in Figs. 2 and 3. From these practically measured voltage equations, the device parameters (E_g, n, and C) of the LED can be extracted.

B. Bidirectional Thermal Resistance Model for Flat LEDs With a Large Surface Area

For a flat LED package with a relatively large surface area, the heat flow from the device junction to the ambient through the phosphor coating and silicone cover cannot be ignored [19].

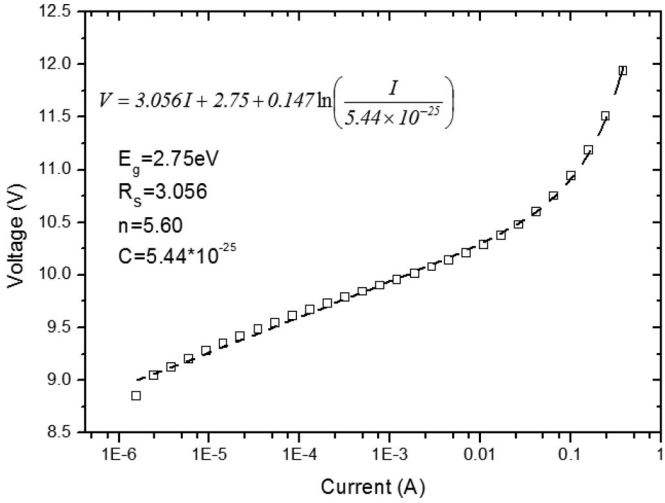

Fig. 2. Measured current versus voltage of the blue LED.

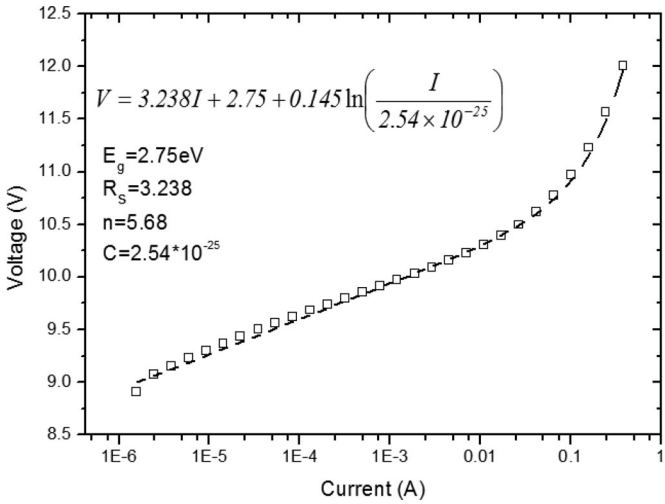

Fig. 3. Measured current versus voltage of the PC white LED.

This means that the bidirectional heat flow on both sides of the flat LED package should be considered. In fact, it will be shown that if such bidirectional heat flow is included, the theoretical prediction of the junction temperature and, thus, the luminous output would be much more accurate. For the samples shown in Fig. 1, two heat flow paths can be considered. First, the heat flow from the junction to the heat sink and then heat sink to the ambient can be, respectively, represented by the junction-to-case thermal resistance $R_{\rm jc}$ and the heat sink thermal resistance $R_{\rm hs}$, which are shown in Fig. 4. Second, the heat flow from the junction to the phosphor coating and the silicone cover should be included. For the blue LED, which has the phosphor coating removed, a thermal resistance $R_{\rm silicone}$ as shown in Fig. 4(a) can be used to represent such a heat flow path. For the PC white LED, such a path is represented by the thermal resistance $R_{\rm silicone}$ in series with the thermal resistance of the phosphor coating $R_{\rm phosphor}$ as shown in Fig. 4(b). The model in Fig. 4(b)

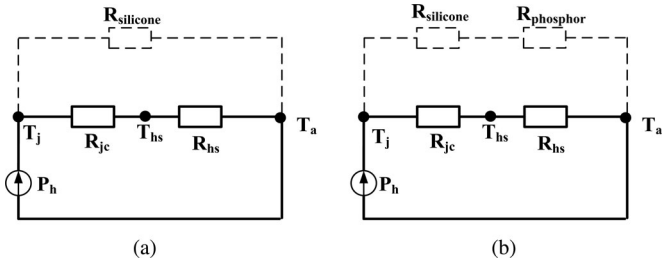

Fig. 4. Bidirectional thermal resistance network of the LED device. (a) Blue LED and (b) PC white LED.

will be used to demonstrate the heat trapping effects of the encapsulation layers in the flat LED package.

Several assumptions were made for the thermal model: 1) perfect contact exists at interfaces between different layers; 2) heat is conducted along the vertical direction in each layer in the thermal model; 3) the spreading resistance among the LED chips is neglected; and 4) thermal radiation is neglected. Based on the above assumptions, the equivalent thermal resistance for blue LED ($R_{\mathrm{jc},b}$) and PC white LED ($R_{\mathrm{jc},w}$) can be expressed as

$$R_{\mathrm{jc},b} = \frac{1}{\frac{1}{R_{\mathrm{silicone}}} + \frac{1}{R_{\mathrm{jc}}+R_{\mathrm{hs}}}}. \tag{4}$$

$$R_{\mathrm{jc},w} = \frac{1}{\frac{1}{R_{\mathrm{phosphor}}+R_{\mathrm{silicone}}} + \frac{1}{R_{\mathrm{jc}}+R_{\mathrm{hs}}}}. \tag{5}$$

In order to determine the equivalent thermal resistance (R_{jc}) of the LED chips in the package, a third LED sample without the phosphor coating and the silicone cover is tested. For a blue LED without the silicone cover, the thermal resistance can be expressed as

$$R_{\mathrm{jc},b'} = \frac{1}{\frac{1}{R_{\mathrm{air}}} + \frac{1}{R_{\mathrm{jc}}}} \approx R_{\mathrm{jc}} \tag{6}$$

where R_{air} is the thermal resistance of air, which is very large as compared with other thermal resistance.

Using the transient thermal tester (T3Ster) LED measurement system, the thermal resistance values of the LED samples 1) without phosphor coating and silicone cover, 2) with silicone cover but without phosphor coating, and 3) with both phosphor coating and silicone cover are measured. The total equivalent thermal resistance for the three samples 1) blue LED without silicone cover $R_{\mathrm{jc},b}{}'$, 2) blue LED with silicone cover $R_{\mathrm{jc},b}$, and 3) PC white LED $R_{\mathrm{jc},w}$ are recorded in Fig. 5. It is noted that $R_{\mathrm{jc},b}$ is smaller than $R_{\mathrm{jc},w}$ because there is no phosphor coating that generates and traps heat when the diode is in operation. In addition, $R_{\mathrm{jc},b}$ is smaller than $R_{\mathrm{jc},b}{}'$ because the total heat loss surface area of the LED chips is much smaller than that of the silicone cover. Based on the thermal equivalent circuits in Fig. 4 and (4)–(6), it can be found that R_{silicone} is about 21.3 °C/W and R_{phosphor} is about 16.8 °C/W.

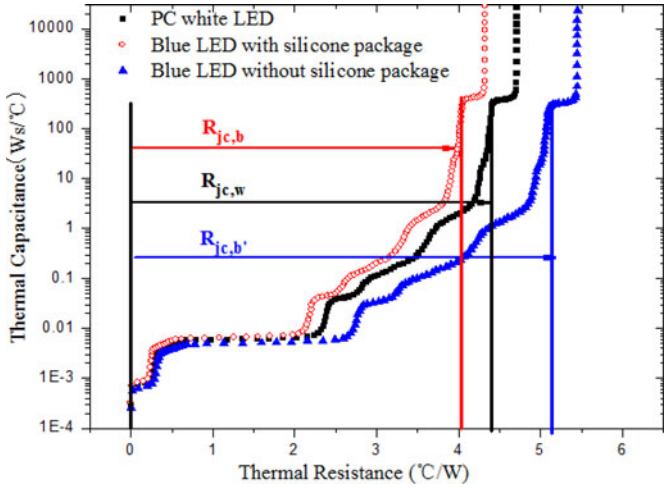

Fig. 5. Thermal resistance and capacitance of the three samples (blue LED without silicone package, blue LED with silicone package, and PC white LED).

C. Electrothermal Model Equations for the Blue LED and the PC LED

Based on the bidirectional thermal resistance network described above, the thermal model for the LED can be expressed as

$$P_{\mathrm{heat}} = \frac{T_j - T_a}{R_{\mathrm{up}}} + \frac{T_j - T_a}{R_{\mathrm{down}}} \tag{7}$$

where R_{up} refers to the total thermal resistance in the heat flow path from the junction through the surface of the LED package to the ambient, and R_{down} refers to the total thermal resistance from the junction through the heat sink to the ambient. Based on (4) and (5), the junction temperature $T_{j,b}$ and $T_{j,w}$ for the blue LED and PC white LED mounted on a heat sink with a thermal resistance R_{hs} can be rewritten as

$$\begin{aligned} T_{j,b} &= T_a + R_{\mathrm{jc},b}P_{h,b} \\ &= T_a + \left(\frac{1}{1/R_{\mathrm{silicone}} + 1/(R_{\mathrm{jc}}+R_{\mathrm{hs}})}\right) k_{h,b} IV \end{aligned} \tag{8}$$

$$\begin{aligned} T_{j,w} &= T_a + R_{\mathrm{jc},w}P_{h,w} \\ &= T_a + \left(\frac{1}{1/(R_{\mathrm{silicone}}+R_{\mathrm{phosphor}}) + 1/(R_{\mathrm{jc}}+R_{\mathrm{hs}})}\right) \\ &\quad \times k_{h,w} IV. \end{aligned} \tag{9}$$

Putting (2) into (8) and (9), $T_{j,b}$ and $T_{j,w}$ can be obtained as

$$\begin{aligned} T_{j,b} &= T_a + R_{\mathrm{jc},b}k_{h,b}I\left[IR_s + \frac{E_g}{q} + \frac{nkT_{j,b}}{q}\ln\left(\frac{I}{C}\right)\right] \\ &= \frac{T_a + k_{h,b}\left(\frac{1}{1/R_{\mathrm{silicone}}+1/(R_{\mathrm{jc}}+R_{\mathrm{hs}})}\right)\left(I^2R_s + I\frac{E_g}{q}\right)}{1 - k_{h,b}\left(\frac{1}{1/R_{\mathrm{silicone}}+1/(R_{\mathrm{jc}}+R_{\mathrm{hs}})}\right)\frac{nk}{q}I\ln\left(\frac{I}{C}\right)} \end{aligned} \tag{10}$$

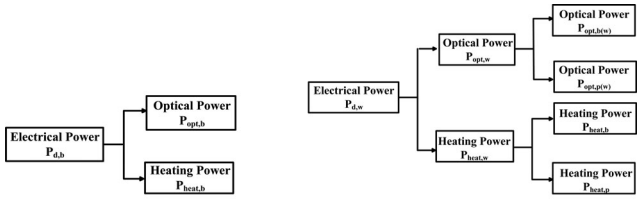

Fig. 6. Energy flow illustration in LED package of a (a) blue LED and a (b) PC white LED.

$$T_{j,w} = T_a + R_{\mathrm{jc},w} k_{h,w} I \left[I R_s + \frac{E_g}{q} + \frac{nkT_{j,w}}{q} \ln\left(\frac{I}{C}\right)\right] = \frac{T_a + k_{h,w}\left(\frac{1}{1/(R_{\mathrm{silicone}}+R_{\mathrm{phosphor}})+1/(R_{\mathrm{jc}}+R_{\mathrm{hs}})}\right)\left(I^2 R_s + I\frac{E_g}{q}\right)}{1 - k_{h,w}\left(\frac{1}{1/(R_{\mathrm{silicone}}+R_{\mathrm{phosphor}})+1/(R_{\mathrm{jc}}+R_{\mathrm{hs}})}\right)\frac{nk}{q} I \ln\left(\frac{I}{C}\right)}. \quad (11)$$

Several important observations should be noted from (10) and (11).

1) Equations (10) and (11) relate the junction temperature ($T_{j,b}$ or $T_{j,w}$) to the forward current *I,* the thermal resistance of the heat sink R_{hs}, the LED device ($R_{\mathrm{jc},b}$ or $R_{\mathrm{jc},w}$), the device package (R_{silicone} and/or R_{phosphor}), and other physical parameters of the device (such as band gap energy E_g, series resistance R_s, and the ideality factor *n*) altogether. It is an equation that integrates the thermal, electrical, and physical characteristics of the LED system altogether.
2) For a given thermal design with a given set of R_{hs} and $R_{\mathrm{jc},b}$ or $R_{\mathrm{jc},w}$, the junction temperature $T_{j,b}$ or $T_{j,w}$ is dependent on the physical parameters such as the bandgap energy E_g, the series resistance R_s, and the ideality factor *n*.
3) The ideality factor *n* is related to the carrier transport, recombination, and resistivity. It has been commonly used as an indicator for device performance. A high ideality factor results in a high junction temperature and, thus, limits the power efficiency.
4) It has been suggested that ideality factor of a diode is dependent on the trap-assisted tunneling and carrier leakage. However, no quantitative modeling has been previously reported to relate the junction temperature to the high ideality factor in LEDs. Therefore, (10) and (11) provides a new formulation linking the junction temperature to the ideality factor.
5) As the ideality factor is associated with a negative term in the denominator of (10) and (11), a large ideality factor will lead to a small value in the denominator, which in turn will result in a higher junction temperature. Therefore, this new equation quantitatively sums up the relationship of junction temperature and ideality factor.

The LED power will be turned into heat (-heat dissipation power P_{heat}) and light (-optical power P_{opt}). Fig. 6(a) and (b) show the power flow structures of the blue LED and the PC white LED, respectively. The power flow structure of the PC white LED is more complicated than that of the blue LED due to the presence of the phosphor coating. In order to evaluate the effects of the phosphor coating, the power of the blue LED and the PC white LED are set to be identical in the analysis. Therefore

$$P_{d,w} = P_{d,b} \quad (12)$$

where $P_{d,w}$ and $P_{d,b}$ are the total electrical LED power of the PC white LED and the blue LED, respectively.

For the blue LED, the heat dissipation coefficient $k_{h,b}$ can be expressed as

$$k_{h,b} = \frac{P_{\mathrm{heat},b}}{P_{d,w}} = 1 - \frac{P_{\mathrm{opt},b}}{P_{d,w}}. \quad (13)$$

For the PC white LED, heat dissipation occurs in both the blue LED and the phosphor coating. Therefore, the heat dissipation coefficient $k_{h,w}$ of the PC white LED is

$$k_{h,w} = \frac{P_{\mathrm{heat},w}}{P_{d,w}} = \frac{P_{\mathrm{heat},b}}{P_{d,w}} + \frac{P_{\mathrm{heat},p}}{P_{d,w}} = 1 - \frac{P_{\mathrm{opt},w}}{P_{d,w}} = \left(1 - \frac{P_{\mathrm{opt},b}}{P_{d,w}}\right) + \left(\frac{P_{\mathrm{opt},b} - P_{\mathrm{opt},b(w)} - P_{\mathrm{opt},p(w)}}{P_{d,w}}\right) \quad (14)$$

where $P_{\mathrm{opt},b}$ is the optical power for the blue LED, $P_{\mathrm{opt},b(w)}$ is the optical power for the blue light of the PC white LED, $P_{\mathrm{opt},p(w)}$ is the optical power for the phosphor light of the PC white LED, $P_{\mathrm{opt},w}$ is the optical power for the PC white LED, $P_{\mathrm{heat},b}$ is the heat dissipation in the blue LED chip, and $P_{\mathrm{heat},p}$ is the heat dissipation in the phosphor layer.

Some energy of the blue light emitted from the blue LED chip is consumed in the phosphor layer, where light scattering, conversion, and absorption occur simultaneously. Therefore, the emitted light of the blue LED chip can be divided into two parts. Part of blue light absorbed by the phosphor layer is converted into yellow light, part of blue light is emitted through the optical cover of the PC white LED package, and the rest is converted into heat. The energy of the converted yellow light dissipates during its propagation in the phosphor layer follows the Lamber–Beer's law [4]. The optical power of generated yellow light within phosphor can propagate in the *z*-direction or in its opposing direction *z* [1]. $P_{\mathrm{opt},p(w)}$ represents the power of the yellow light in the *z*-direction (light emitting outside package), and $P_{\mathrm{opt},p(w)-}$ represents the opposite direction, as shown in Fig. 7. If Δz is close to zero, based on energy balance across the phosphor, the power gradient [17] of the yellow light in the phosphor layer can be expressed as

$$\frac{dP_{\mathrm{opt},p(w)-}}{dz} = \alpha_P \times P_{\mathrm{opt},p(w)-} - \frac{1}{2}\beta \times P_{\mathrm{opt},b(w)} \quad (15)$$

$$\frac{dP_{\mathrm{opt},p(w)}}{dz} = -\alpha_P \times P_{\mathrm{opt},p(w)} + \frac{1}{2}\beta \times P_{\mathrm{opt},b(w)} \quad (16)$$

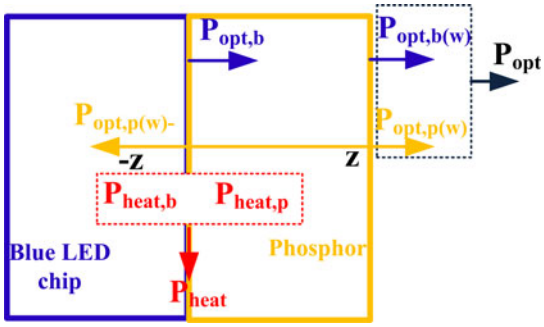

Fig. 7. Optical transfer in the phosphor and blue LED chip layer.

and the power gradient for the blue light in phosphor layer is

$$\frac{dP_{\mathrm{opt},b(w)}}{dz} = -\alpha_B \times P_{\mathrm{opt},b(w)} \tag{17}$$

where α_P is a coefficient of yellow light absorption in the silicone cover, α_B is a coefficient of blue light absorption in the phosphor layer, β is a conversion coefficient for blue light converting to yellow light through the phosphor layer, and z is the displacement in the z-direction. $P_{\mathrm{opt},p(w)}$ is the optical power of the yellow light of the PC white LED in the z-direction. It represents the light power emitting out of the PC white LED package.

The optical power of blue light at $z = 0$ is $P_{\mathrm{opt},b}$, the optical power of blue light at $z = h$ (where h is the thickness of phosphor layer) is $P_{\mathrm{opt},b(w)}$, and the optical power of phosphor light at $z = 0$ is zero. Blue light and yellow light are slightly absorbed by silicone, due to the high transmittance of silicone encapsulating [8]. It is assumed that the yellow light absorbed by silicone α_{P} and the light scattered back by the phosphor particles is negligible [17]. According to the boundary conditions, the above equations can be rewritten as

$$P_{\mathrm{opt},b(w)} = P_{\mathrm{opt},b} \times e^{-\alpha_B h} \tag{18}$$

$$P_{\mathrm{opt},p(w)} = \frac{\beta \times P_{\mathrm{opt},b}}{2\alpha_B}\left(1 - e^{-\alpha_B h}\right). \tag{19}$$

So, the heating power generated by the phosphor $P_{\mathrm{heat},p}$ can be given as

$$\begin{aligned}\frac{P_{\mathrm{heat},p}}{P_{d,w}} &= \left(\frac{P_{\mathrm{opt},b} - P_{\mathrm{opt},b(w)} - P_{\mathrm{opt},p(w)}}{P_{d,w}}\right) \\ &= \left(\frac{P_{\mathrm{opt},b} - P_{\mathrm{opt},b(w)} - P_{\mathrm{opt},p(w)}}{P_{\mathrm{opt},b}}\right)\frac{P_{\mathrm{opt},b}}{P_{d,w}} \\ &= \left(1 - \frac{P_{\mathrm{opt},b(w)}}{P_{\mathrm{opt},b}} - \frac{P_{\mathrm{opt},p(w)}}{P_{\mathrm{opt},b}}\right)(1 - k_{h,b}) \\ &= \left[1 - \frac{\beta}{2\alpha_B} - e^{-\alpha_B h}\left(1 - \frac{\beta}{2\alpha_B}\right)\right](1 - k_{h,b}).\end{aligned} \tag{20}$$

Then, k_h of the white LED in (20) can be obtained as

$$k_{h,w} = \left[2 - \frac{\beta}{2\alpha_B} - e^{-\alpha_B h}\left(1 - \frac{\beta}{2\alpha_B}\right)\right](1 - k_{h,b}). \tag{21}$$

Based on (21), several important points should be noted.

1) The heat dissipation coefficient of the PC white LED $k_{h,w}$ is related to the heat dissipation coefficient of the blue chip $k_{h,b}$, the absorption coefficient of blue light on the phosphor layer α_B, the conversion coefficient of blue light converting into yellow light β, and the phosphor thickness h.
2) LED device manufacturers can use parameters such as α_B, β, and h in (21) to quantify their PC white LED devices and estimate the heat generated by the phosphor layer. By minimizing the second term on the right-hand side of (21), the power loss and temperature in the phosphor layer can be reduced, leading to an improvement in reliability and efficiency of future PC white LEDs.
3) For a given phosphor material, the heating power generated by the phosphor layer is dependent on the phosphor thickness. A thicker phosphor layer leads to more photon energy absorption and heat dissipation in the phosphor layer. However, such phosphor layer cannot be too thin; otherwise, most of the blue light will escape through the layer without conversion to yellow light. Further study is needed to optimize such thickness.

D. Photoelectrothermal Model Based on Multiphysical Properties

Based on the original PET theory [9], [10], the luminous flux ϕ_{v} of N LED devices is

$$\begin{aligned}\phi_v = NEP_d = {} & NE_0\{[1 + k_e(T_a - T_0)]P_d \\ & + k_e k_h (R_{\mathrm{jc}} + NR_{\mathrm{hs}})P_d^2\}.\end{aligned} \tag{22}$$

In general, the luminous flux can be expressed in the general form of $\phi_v = \alpha_1 P_d - \alpha_2 P_d^2$, where α_1 and α_2 are two positive system coefficients. It should be noted that the LED power P_d is used in the luminous flux equation because it includes the effects of both of the junction temperature and the LED current [18]. These two coefficients are not necessarily constant throughout the operating power range. The coefficient α_2 usually increases with increasing P_d, so that the luminous flux equation is an asymmetric parabolic function of the LED power.

According to [10], where luminous efficacy E with junction temperature and electrical power can be expressed as

$$\begin{aligned}E = {} & E_0[1 + k_e(T_j - T_0)] = E_0[1 + k_e(T_a - T_0) \\ & + k_e k_h (R_{\mathrm{jc}} + NR_{\mathrm{hs}})P_d] \\ = {} & E_0[1 + k_e(T_a - T_0) + k_e(1 - \eta_w)(R_{\mathrm{jc}} + NR_{\mathrm{hs}})P_d] \\ = {} & E_0\{1 + k_e(T_a - T_0) \\ & + k_e\left[1 - \frac{(\alpha T_j + \beta)\left(\chi P_d^2 + \delta P_d + \gamma\right)}{\mu}\right] \\ & \times (R_{\mathrm{jc}} + NR_{\mathrm{hs}})P_d\}.\end{aligned} \tag{23}$$

In order to simplify above expression, the wall-plug efficiency η_w with electrical power P_d can be expressed as first-order regression

$$E = E_0\{1 + k_e(T_a - T_0) + k_e\left[1 - \mu'\left(\alpha' T_j + \beta'\right)\left(\delta' P_d + \gamma'\right)\right] \times (R_{\rm jc} + NR_{\rm hs})P_d\} \quad (24)$$

where α', β', δ', γ', and μ' are calibrated coefficients for η_w with electrical power and the junction temperature. Therefore, (23) can be rewritten as

$$E = E_0\{1 + k_e(T_a - T_0) + k_e(R_{\rm jc} + NR_{\rm hs})P_d - k_e(R_{\rm jc} + NR_{\rm hs})\left(\delta' P_d^2 + \gamma' P_d\right)\mu'\left(\alpha' T_j + \beta'\right)\}. \quad (25)$$

Based on (25), several important points should be noted

1) The luminous efficacy *E* is related to the electrical power P_d, the junction temperature T_j, thermal resistance of device $R_{\rm jc}$, thermal resistance of heat sink $R_{\rm hs}$, the LED device number *N*, and the coefficients α', β', δ', γ', and μ'.
2) It is noted that the coefficients α', β', δ', and γ' can be extracted from a series measurement of η_w with junction temperature and electrical power [10]. The coefficients $\alpha'$and δ' are both negative.
3) For a given thermal design with a given set of $R_{\rm hs}$ and $R_{\rm jc}$, the luminous efficacy *E* is dependent on the electrical power P_d. In general, *E* decreases with increasing power P_d and the relationship is close to but not exactly a straight line, as will be shown in Fig. 12(a) and 13(a).
4) If space for the heat sink is not an issue, a big heat sink with low $R_{\rm hs}$ should always be selected for the LED system in order to effectively reduce the reduction of the luminous efficacy *E* at higher temperature.
5) The slope value of luminous efficacy *E* versus junction temperature T_j is dependent on the coefficient of $-k_e(R_{\rm jc} + NR_{\rm hs})\left(\delta' P_d^2 + \gamma' P_d\right)\mu'\alpha'$. The factor $(R_{\rm jc} + NR_{\rm hs})$ decreases with $R_{\rm hs}$, and the factor $(\delta' P_d^2 + \gamma' P_d)$ increases initially with P_d, and then reduce significantly with increasing P_d due to negative value of δ'. Therefore, the slope of E–T_j depends on the heat sink's thermal resistance.

The electrical power expressed in (3) with the multiphysical characteristics ($E_g, n, R_s,$ and C) can be used with (22) to determine the total luminous output, which is given as

$$\phi_v = NEP_d = NE_0\left\{\begin{array}{l}\left[1 + k_e\left(T_a - T_0\right)\right] \\ \quad \times\left(I^2 R_s + I\frac{E_g}{q} + I\frac{nkT_j}{q}\ln\left(\frac{I}{C}\right)\right) \\ +k_e k_h\left(R_{\rm jc} + NR_{\rm hs}\right) \\ \quad \times\left(I^2 R_s + I\frac{E_g}{q} + I\frac{nkT_j}{q}\ln\left(\frac{I}{C}\right)\right)^2\end{array}\right\} \quad (26)$$

Equation (26) relates the luminous flux ϕ_v to the current *I*, the thermal resistance of heat sink $R_{\rm hs}$, the LED $R_{\rm jc}$, the junction temperature of LED T_j, and other physical parameters of LED ($E_g, n, R_s,$ and C) altogether. It is important to note that the junction temperature of the blue and PC white LEDs can also be, respectively, replaced by the thermal models in (8) and (9).

Based on (4) and (5), the PET theory for the *N* blue LEDs can be developed as

$$\phi_{v,b} = NEP_{d,b} = NE_0\left\{\begin{array}{l}\left[1 + k_e\left(T_a - T_0\right)\right]\left(I^2 R_s + I\frac{E_g}{q} + I\frac{nkT_{j,b}}{q}\ln\left(\frac{I}{C}\right)\right) \\ \quad + k_e k_{h,b}\left(\frac{1}{N/R_{\rm silicone} + 1/(N/R_{\rm jc} + NR_{\rm hs})}\right) \\ \quad \times\left(I^2 R_s + I\frac{E_g}{q} + I\frac{nkT_{j,b}}{q}\ln\left(\frac{I}{C}\right)\right)^2\end{array}\right\}. \quad (27)$$

Putting (16) into (18), the PET theory for the *N* PC white LED can be expressed as

$$\phi_{v,w} = NEP_{d,w} = NE_0\left\{\begin{array}{l}\left[1 + k_e\left(T_a - T_0\right)\right]\left(I^2 R_s + I\frac{E_g}{q} + I\frac{nkT_{j,w}}{q}\ln\left(\frac{I}{C}\right)\right) \\ \quad + k_e\left(k_{h,b} + \left[1 - \frac{\beta}{2\alpha_B} - e^{-\alpha_B h}\left(1 + \frac{\beta}{2\alpha_B}\right)\right]k_{h,b}\right) \\ \quad \times\left(\frac{1}{N/(R_{\rm silicone} + R_{\rm phosphor}) + 1/(N/R_{\rm jc} + R_{\rm hs})}\right) \\ \quad \times\left(I^2 R_s + I\frac{E_g}{q} + I\frac{nkT_{j,w}}{q}\ln\left(\frac{I}{C}\right)\right)^2\end{array}\right\}. \quad (28)$$

Several important observations can be made from (28)

1) Equation (28) not only relates the luminous flux $\phi_{v,w}$ to the injection current of the PC white LED *I,* the thermal resistance of the heat sink $R_{\rm hs}$, the device $R_{\rm jc}$, and the package $R_{\rm silicone}/R_{\rm phosphor}$, but it also includes the multiphysical characteristics of the device ($E_g, n, R_s,$ and C) and the phosphor characteristics ($\alpha_B, \beta,$ and h). It is a model that integrates the photometric, electrical, thermal, and physical aspects of the PC white LED system altogether.
2) As k_e is negative and less than 1, when the diode current is increased from zero, the luminous flux is increased quasi-linearly in the low-current region and after reaching the maximum point at current I^*, the luminous flux will decrease as current increases according to the LED system behavior. If the heat dissipation coefficient is increased by the inclusion of the phosphor materials or its fabricated process for the PC white LED, the second item will be increased, and I^* will shift to a lower value. This leads to the possibility that I^* may occur at a current level lower than the rated current of the LED.
3) For a given thermal design and set of $R_{\rm hs}$ and $R_{{\rm jc},w}$, one should expect that I^* could be shifted to a higher current level if there is a reduction in photon energy absorption occurring inside the phosphor layer (i.e., enhancement on the conversion coefficient of blue light converting into yellow light, reduction in phosphor thickness, and absorption coefficient).

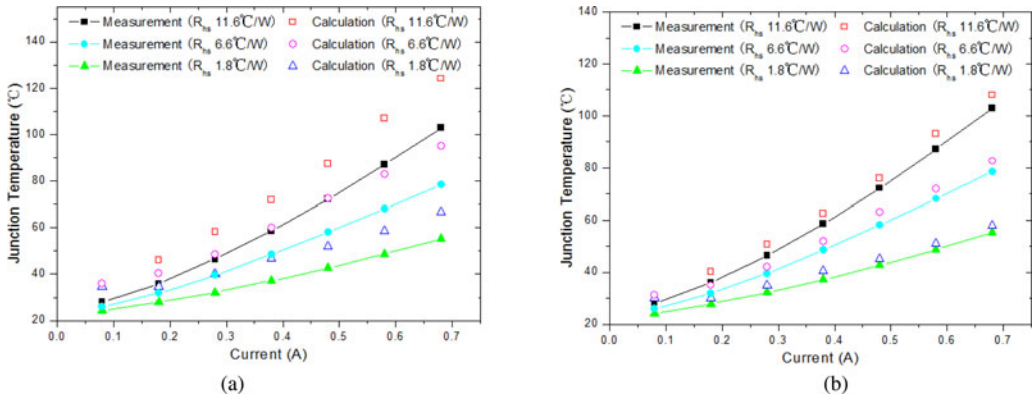

Fig. 8. Calculated and measured junction temperature versus injection current of the blue LED mounted on three different heat sinks. (a) "unidirectional" thermal model (b) "bidirectional" thermal model

III. Experimental Verification

The blue LED and PC white LEDs shown in Fig. 1 have been used for practical evaluation. For a fair comparison, the same input power is used for the blue LED sample and for the PC white LED (i.e., $P_{d,b} = P_{d,w}$) as suggested in (12). Each LED package has 16 chips mounted on the aluminum substrate with silver paste used for attaching the die. There are four chips in series connection in a string. Four of these strings are connected in parallel to form the LED. The dimension of each LED chip is 0.55 mm $\times$ 0.96 mm, and the silver film (black area) is 9.83 mm $\times$ 11.45 mm. The thickness of the phosphor coating is 0.5 mm. The optical measurements of the LED samples are performed under steady-state thermal and electrical conditions using the PMS-50 spectrophotocolorimeter with an integrating sphere (measured after 20 minutes of operation at different electrical power levels and at an ambient temperature of 20 °C). The voltage change of the LED devices with temperature variations are captured using the T3Ster. Besides the combined thermal and optical measurements, the temperature dependence of the optical power and the wall-plug efficiency η_w of the LED are also recorded. The T3Ster captures the thermal transient response in real time, records the cooling/heating curve, and then evaluates the cooling/heating curves for plotting the thermal characteristics. The heating current for the samples is 0.4 A and the heating/cooling time is 20 minutes. The measured current is 5 mA. For voltage-temperature-sensitive parameter calibration, a small current of 5 mA is applied to a temperature-controlled heat sink (at different ambient temperature values: 25, 35, 45, and 55 °C) under a pulsed current injection mode with a small duty cycle. The thermal resistance of the LED package could be extracted using the thermal structure function, which is based on the distribution *RC* networks [11], [16].

A. Junction Temperature

According to (2) and the measured current–voltage curves in Figs. 2 and 3, the ideality factor of the blue LED is around 5.68, and that for the white LED is around 5.60. The bidirectional thermal resistance model is compared with the traditional unidirectional thermal resistance model (i.e., thermal equivalent circuits in Fig. 4(a) and (b) without the dotted branches). The LED samples are tested on three different heat sinks. Fig. 8(a) and (b) shows the theoretical values of the junction temperature of the blue LED sample based on the unidirectional and bidirectional models, respectively. The corresponding practical measurements are also plotted in the figures. While both models give the correct trend of the characteristics, the bidirectional thermal model offers a more accurate prediction than the unidirectional model. Similar sets of junction temperature results of the PC white LED sample are also used for the comparison of both the unidirectional and bidirectional models. The results based on the unidirectional model are shown in Fig. 9(a), while those based on the bidirectional model are shown in Fig. 9(b). It can be seen that the bidirectional thermal model, which includes the heat flow through the surface area of the LED sample, offers a better prediction than the unidirectional model. For the blue LED sample mounted on different heat sinks, the average deviation between the unidirectional model and the measurement is about 13.5% and that between the bidirectional model and the measurement is 7.9%. For the white LED sample, the average deviation between the unidirectional model and the measurement is about 11.7% and that between the bidirectional model and the measurement is 5.2%. Therefore, the results in Figs. 8 and 9 confirm the validity of the bidirectional thermal model. Theoretical results based on the bidirectional thermal model are used for discussion hereafter. The peak wavelength of the blue LED increases from about 451.2 nm at the junction temperature of 39 °C to about 454.7 nm at junction temperature of 108 °C. The peak wavelength and correlated color temperature of the PC white LED increases from about 451.0 nm and 2954 K, respectively, at the junction temperature of 42 °C to about 455.4 nm and 3136 K, respectively, at the junction temperature of 127 °C.

B. Heat Dissipation Coefficient k_{h}

The heat dissipation coefficient is a measure of the proportion of the total input power that turns into heat dissipation in

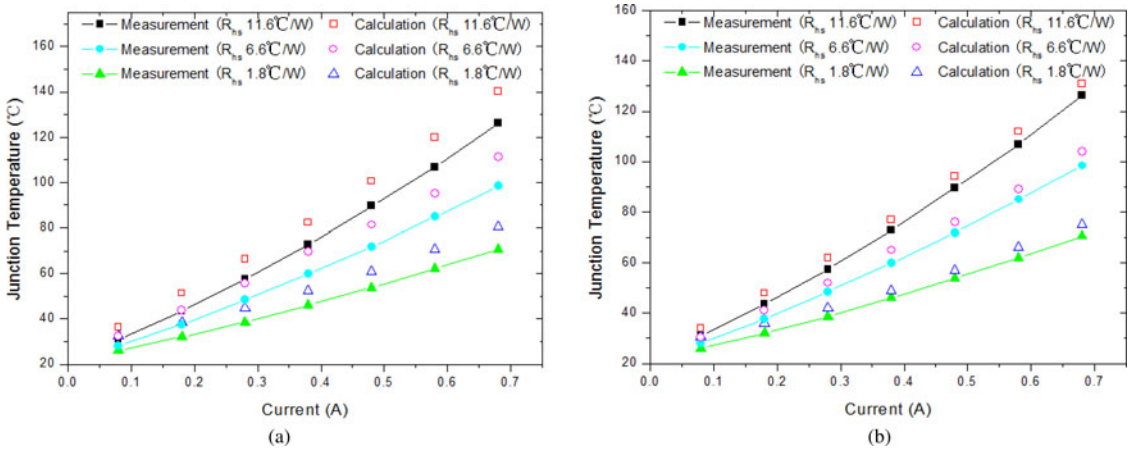

Fig. 9. Calculated and measured junction temperature versus injection current of the PC white LED mounted on three different heat sinks. (a) "unidirectional" thermal model (b) "bidirectional" thermal model

TABLE I
LED SYSTEM PARAMETERS

	E_0 (lm/W)	k_h (*I*:0.05A–0.7A)	k_e (*I*:0.05A–0.7A)	$R_{\rm jc}$ (°C/W)	$R_{\rm hs}$ (°C/W)	N	T_0 (°C)	T_a (°C)
Blue LED	18	0.496 to 0.551	−0.0016 to −0.0021	4.03	1.8 to 11.6	1	25	23
PC White LED	126	0.562 to 0.723	−0.0028 to −0.0036	4.45	1.8 to 11.6	1	25	23

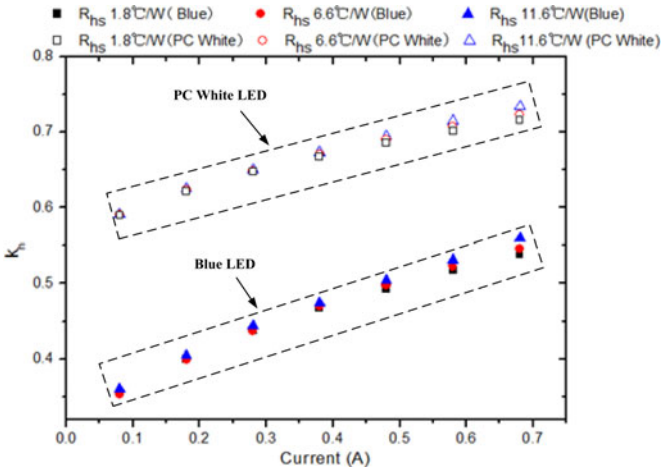

Fig. 10. Measured k_h versus injection current of the blue and PC white LEDs with different heat sinks.

the LED. The experimental results of the two LED samples are plotted in Fig. 10. For the blue LED sample, only a fraction (34–56%) of the electrical energy input into the blue LED is converted to heat. But for the PC white LED sample, the heat dissipation is increased to the range of 59–73%. This increase is caused by the phosphor coating. As shown in (21), the increase in heat dissipation for the PC white LED could be caused by the phosphor characteristics (α_B, β, and h). So, it is important to understand the photon energy loss inside the phosphor layer so as to predict accurate thermal characteristics of the PC white LED.

For the PC white LED in the experiment, the thickness h is around 0.5 mm. The photon absorption coefficient (α_B) by the phosphor can be calculated based on absorption spectrum provided by phosphor manufacturers. The calculated result for α_B is around 28.3 $\rm cm^{-1}$. The spectral power distribution of the PC white LED is measured with the integrating sphere system. The optical power for yellow light of the PC white LED $P_{{\rm opt},p(w)}$ and the optical power for blue light of the blue LED $P_{{\rm opt},b}$ can be determined by integrating the power distribution curve. The measured results for $P_{{\rm opt},p(w)}$ and $P_{{\rm opt},b}$ are about 1.62 and 2.47 W, respectively. Based on (19), the conversion coefficient (β) for the blue light converting into yellow light is calculated as 48.7 $\rm cm^{-1}$.

Based on known phosphor characteristics (α_B, β, and h) and $k_{h,b}$ of the blue LED, the heat dissipation coefficient of the PC white LED as a function of current is calculated using (21) and is plotted in Fig. 11. In general, the calculated results are consistent with the practical measurements given in Fig. 10. Relatively large errors occur at the low current range (<0.2 A) because the relative power measurement errors tend to be large when the input power is very small. It is noted that the calculated k_h curves tend to be slightly smaller than the measurements. The reason for this trend is that the simplified phosphor modeling in (19) ignores the yellow light absorption in silicone layer and the light scattered back by the phosphor particles. In addition,

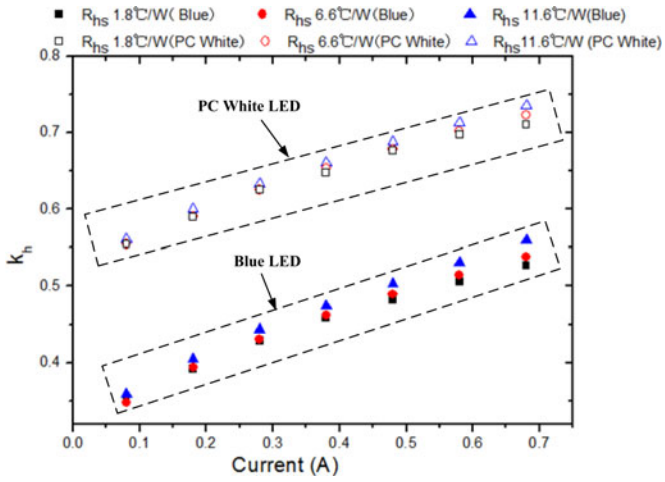

Fig. 11. Calculated k_h versus current of the blue and the PC white LED with different heat sinks.

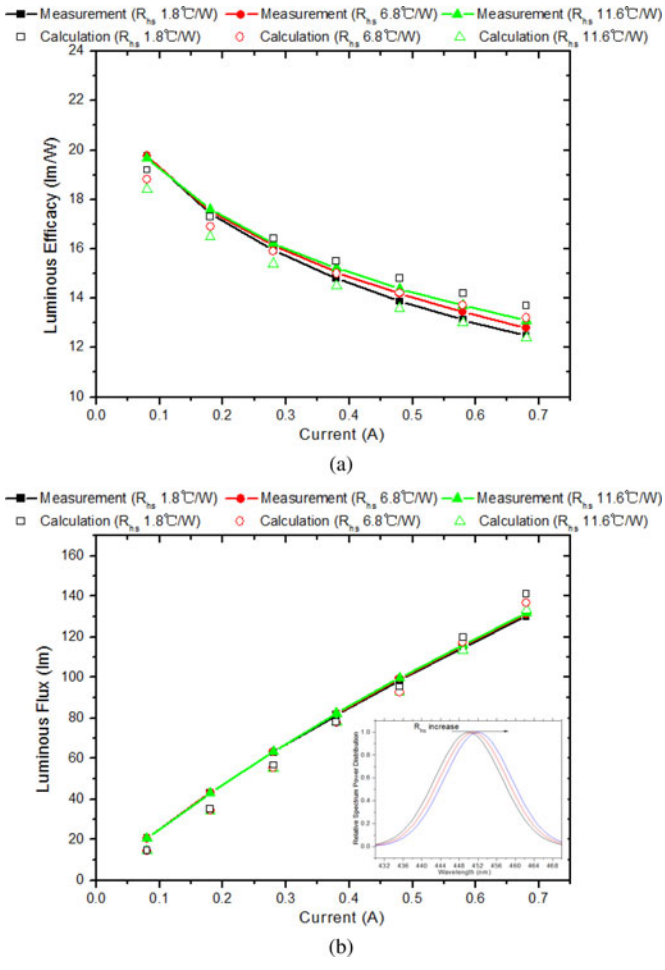

Fig. 12. (a) Calculated and measured luminous efficacy versus current of the blue LED on three different heat sinks. (b) Calculated and measured luminous flux versus current of the blue LED on three different heat sinks.

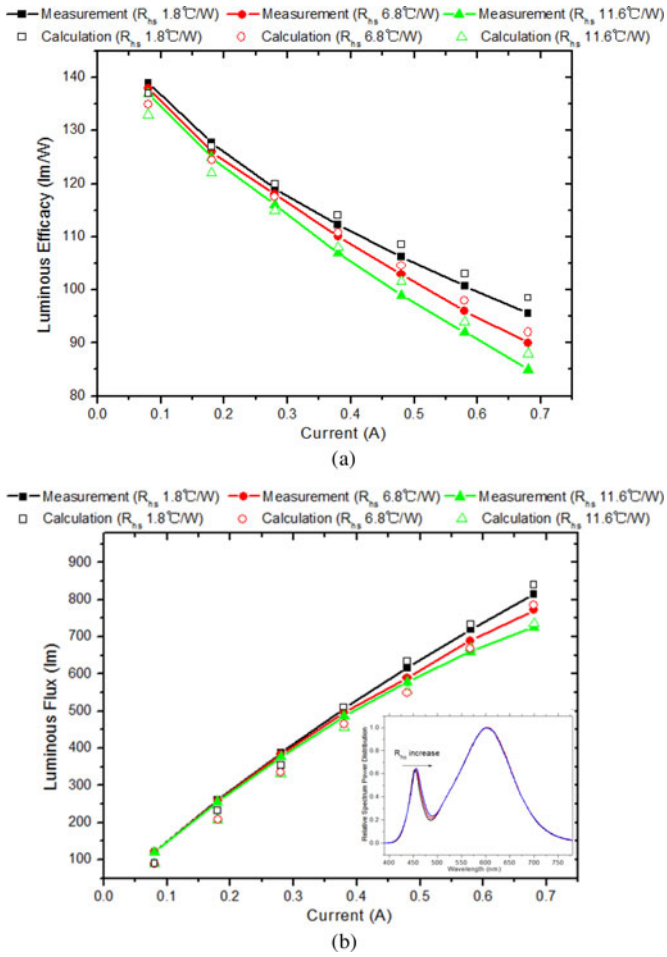

Fig. 13. (a) Calculated and measured luminous efficacy versus current of the PC white LED on three different heat sinks. (b) Calculated and measured luminous flux versus current of the PC white LED on three different heat sinks.

it is assumed that blue light absorption in the phosphor layer is constant among different wavelengths.

C. Luminous Output

Based on (25), the calculated luminous efficacy curves are plotted with the measured results in Fig. 12(a) as functions of the current of the blue LED. The luminous efficacy decreases with increasing current, and the negative slope of the curve changes with the heat sink thermal resistance. Based on (27), the calculated luminous flux curves are plotted along with the measured flux as functions of the current in Fig. 12(b). The system parameters are shown in Table I. Unlike the general trend that the luminous flux–current curve of a white LED should follow an asymmetric parabolic curve when the LED current (and power) increases, the measured luminous flux for the blue LED is almost linear even with increasing heat sink's thermal resistance. The luminous flux of the blue LED is dependent on the spectral power distribution. The response of human eyes is represented by the luminosity function. Wavelengths of light near the peak of the human eye's response (683 lm/W at 555 nm)

contribute more strongly to luminous flux than those far away from the peak. As shown in the insert in Fig. 12(b), the blue color spectrum exhibits red shift and becomes closer to the maximum region of human eye's response curve when the thermal resistance of heat sink increases. This is the reason for the luminous flux–current curve being fairly linear even with increasing $R_{\rm hs}$. Based on (28), the calculated luminous flux and luminous efficacy curves are plotted along with the measurements in Fig. 13. The calculated results are in good agreement with the measurements. These results confirm that the bidirectional thermal model can provide accurate predictions in the framework of the PET theory.

IV. Conclusion

As more modern high-power LED packages are based on the multiple-chip structures with large surface areas, it is necessary to include the heat flow path through the top surface of the LED package. In this paper, a bidirectional thermal resistance model has been developed to predict the effects caused by the phosphor coating on the thermal and luminous performance of white LED devices. The derived bidirectional thermal model given in (5) leads to a more accurate junction temperature equation (9) for the PC white LED. Such model equations can be used in the framework of the PET theory for LED system analysis, which successfully leads to the quantification of the increase in heat dissipation coefficient caused by the phosphor coating in (21). Both the theoretical prediction and practical measurements have confirmed that the phosphor coating could increase the heat dissipation coefficient significantly. The proposed model is a multiphysical one that provides physical insights for researchers and manufacturers. It can be used for analyzing the performance of LED structures in the context of a system, incorporating the interactions of heat, light, and power. The parameters adopted in the model allow LED manufacturers to use as indicators and design parameters for the merits of the devices. The analytical approach also provides application engineers a systematic tool to accurately predict the luminous performance of LED systems in the design stage.

References

[1] M. Huang and L. Yang, "Heat generation by the phosphor layer of high-power white LED emitters," *IEEE Photon. Technol. Lett.*, vol. 25, no. 14, pp. 1317–1320, Jul. 2013.

[2] J. C. Hsieh, D. T. W. Lin, and C. H. Cheng, "Optimization of thermal management by integration of an SCGM, a finite-element method, and an experiment on a high-power LED array," *IEEE Trans. Electron Devices*, vol. 58, no. 4, pp. 1141–1148, Apr. 2011.

[3] T. Tamura, T. Setomoto, and T. Taguchi, "Illumination characteristics of lighting array using 10 candela-class white LEDs under AC 100 V operation," *J. Luminescence*, vol. 87–89, pp. 1180–1182, May 2000.

[4] F. P. Incropera and D. P. Dewitt, *Fundamentals of Heat and Mass Transfer*, 5th ed. New York, NY, USA: Wiley, 2002, Ch. 13, pp. 821–822.

[5] S. Y. R. Hui, S. N. Li, X. H. Tao, W. Chen, and W. M. Ng, "A novel passive offline LED driver with long lifetime," *IEEE Trans. Power Electron.*, vol. 25, no. 10, pp. 2665–2672, Oct. 2010.

[6] X. Ruan, B. Wang, K. Yao, and S. Wang, "Optimum injected current harmonics to minimize peak-to-average ratio of LED current for electrolytic capacitor-less AC–DC drivers," *IEEE Trans. Power Electron.*, vol. 26, no. 7, pp. 1820–1825, Jul. 2011.

[7] M. Arias, D. M. Fernandez, D. G. Lamar, D. Balocco, A. A. Diallo, and J. Sebastian, "High-efficiency asymmetrical half-bridge converter without electrolytic capacitor for low-output-voltage AC–DC LED drivers," *IEEE Trans. Power Electron.*, vol. 28, no. 5, pp. 2539–2550, May 2013.

[8] Y. H. Lin, J. P. You, Y. C. Lin, N. T. Tran, and F. G. Shi, "Development of high-performance optical silicone for the packaging of high-power LEDs," *IEEE Trans. Compon. Packag. Technol.*, vol. 33, no. 4, pp. 761–766, Dec. 2010.

[9] S. Y. R. Hui and Y. X. Qin, "A general photo-electro-thermal theory for light-emitting-diode (LED) systems," *IEEE Trans. Power Electron.*, vol. 24, no. 8, pp. 1967–1976, Aug. 2009.

[10] S. Y. R. Hui, H. T. Chen, and X. H. Tao, "An extended photoelectrothermal theory for LED systems-A tutorial from device characteristic to system design for general lighting [invited paper]," *IEEE Trans. Power Electron.*, vol. 27, no. 1, pp. 4571–4583, Nov. 2012.

[11] G. Farkas, Q. V. V. Vader, A. Poppe, and G. Bognár, "Thermal investigation of high power optical devices by transient testing," *IEEE Trans. Compon. Packag. Technol.*, vol. 28, no. 1, pp. 45–50, Mar. 2005.

[12] S. C. Tan, "General n-level driving approach for improving electrical-to-optical energy-conversion efficiency of fast-response saturable lighting devices," *IEEE Trans. Ind. Electron.*, vol. 57, no. 4, pp. 1342–1353, Apr. 2010.

[13] K. H. Loo, Y. M. Lai, S. C. Tan, and C. K. Tse, "Stationary and adaptive color-shift reduction methods based on the bilevel driving technique for phosphor-converted white LEDs," *IEEE Trans. Power Electron.*, vol. 26, no. 7, pp. 1943–1953, Jul. 2011.

[14] K. H. Loo, Y. M. Lai, S. C. Tan, and C. K. Tse, "On the color stability of phosphor-converted white LEDs under dc, pwm, and bilevel drive," *IEEE Trans. Power Electron.*, vol. 27, no. 2, pp. 974–984, Feb. 2012.

[15] H. Ye, S. W. Koh, G. Yuan, H. V. Zeijl, A. W. J. Gielen, S. W. R. Lee, and G. Q. Zhang, "Electrical-thermal-luminous-chromatic model of phosphor-converted white light-emitting diodes," *Appl. Therm. Eng.*, vol. 63, no. 2, pp. 588–597, Feb. 2014.

[16] A. Poppe, Y. Zhang, J. Wilson, G. Farkas, P. Szabó, J. Parry, M. Rencz, and V. Székely, "Thermal measurement and modelling of multi-die packages," *IEEE Trans. Compon. Packag. Technol.*, vol. 32, no. 2, pp. 484–492, Jun. 2009.

[17] D. Y. Kang, E. Wu, and D. M. Wang, "Modeling white light-emitting diodes with phosphor layers," *Appl. Phys. Lett.*, vol. 89, no. 23, pp. 231102–1–231102-3, Dec. 2006.

[18] H. T. Chen, X. H. Tao, and S. Y. R. Hui, "Estimation of optical power and heat dissipation coefficient for the photo-electro-thermal theory for LED systems," *IEEE Trans. Power Electron.*, vol. 27, no. 4, pp. 2176–2183, Apr. 2012.

[19] E. Juntunen, O. Tapaninen, A. Sitomaniemi, and V. Heikkinen, "Effect of phosphor encapsulant on the thermal resistance of a high-power COB LED module," *IEEE Trans. Compon., Packag. Manuf. Technol.*, vol. 3, no. 7, pp. 1148–1154, Jul. 2013.

Huan Ting Chen (M'13) received the Ph.D. degree in radio physics from Xiamen University, Xiamen, China, in 2010. He was a Joint Ph.D. student at the Light & Lighting Laboratory, Catholic University College Ghent, Ghent, Belgium, from November 2009 to May 2010.

He was a Senior Research Associate in the Department of Electronic Engineering, City University of Hong Kong, Hong Kong, in 2011. He is currently a Postdoctoral Fellow in the Department of Electrical and Electronic Engineering, The University of Hong Kong, Hong Kong. His research interests include solid-state lighting theory and technology.

Siew-Chong Tan (S'00–M'06–SM'11) received the B.Eng. (Hons.) and M.Eng. degrees in electrical and computer engineering from the National University of Singapore, Singapore, in 2000 and 2002, respectively, and the Ph.D. degree in electronic and information engineering from the Hong Kong Polytechnic University, Hong Kong, in 2005.

From October 2005 to May 2012, he was a Research Associate, Postdoctoral Fellow, Lecturer, and Assistant Professor in the Department of Electronic and Information Engineering, Hong Kong Polytechnic University, Hong Kong. From January to October 2011, he was a Senior Scientist in Agency for Science, Technology and Research, Singapore. He is currently an Associate Professor in the Department of Electrical and Electronic Engineering, The University of Hong Kong, Hong Kong. He was a Visiting Scholar at Grainger Center for Electric Machinery and Electromechanics, University of Illinois at Urbana-Champaign, Champaign, Illinois, USA, from September to October 2009, and an Invited Academic Visitor of Huazhong University of Science and Technology, Wuhan, China, in December 2011. His research interests include the areas of power electronics and control, LED lightings, smart grids, and clean energy technologies. He is a coauthor of the book *Sliding Mode Control of Switching Power Converters: Techniques and Implementation* (Boca Raton, FL, USA: CRC, 2011).

Dr. Tan serves extensively as a Reviewer for various IEEE/IET transactions and journals on power, electronics, circuits, and control engineering.

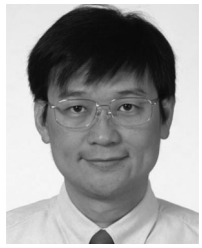

S. Y. R. Hui (M'87–SM'94–F'03) received the B.Sc. (Eng.) Hons. from the University of Birmingham, Birmingham, U.K., in 1984, and the D.I.C. and Ph.D. degrees from Imperial College London, London, U.K., in 1987.

He has previously held academic positions at the University of Nottingham, Nottingham, U.K., from 1987 to 1990, University of Technology, Sydney, Australia from 1991 to 1992, University of Sydney, Sydney, Australia from 1992 to 1996, City University of Hong Kong, Kowloon Hong Kong, from 1996 to 2011. He is currently holds the Chair Professorships at the University of Hong Kong and the Imperial College London. He has published more than 200 technical papers, including more than 170 refereed journal publications and book chapters. More than 55 of his patents have been adopted by industry.

Dr. Hui has been an Associate Editor of the IEEE TRANSACTIONS ON POWER ELECTRONICS since 1997 and an Associate Editor of the IEEE TRANSACTIONS ON INDUSTRIAL ELECTRONICS since 2007. He has been appointed twice as an IEEE Distinguished Lecturer by the IEEE Power Electronics Society in 2004 and 2006. He served as an AdCom Member of the IEEE Power Electronics Society and was the Chairman of its Constitution and Bylaws Committee from 2002 to 2010. He received the Excellent Teaching Award in 1998 and the Earth Champion Award in 2008. He received an IEEE Best Paper Award from the IEEE IAS Committee on Production and Applications of Light in 2002, and two IEEE Power Electronics Transactions Prize Paper Awards for his publications on Wireless Charging Platform Technology in 2009 and on LED system theory in 2010. His inventions on wireless charging platform technology underpin key dimensions of Qi, the world's first wireless power standard, with freedom of positioning and localized charging features for wireless charging of consumer electronics. In November 2010, he received the IEEE Rudolf Chope R&D Award from the IEEE Industrial Electronics Society, the IET Achievement Medal (The Crompton Medal), and was elected to the Fellowship of the Australian Academy of Technological Sciences and Engineering. He is the recipient of the 2015 IEEE William E. Newell Award.